Title: Distinct material properties of sugar-glasses correlate with anhydrobiosis *in vitro* and *in vivo*

Authors
John F. Ramirez[a], U.G.V.S.S. Kumara[a], Navamoney Arulsamy[b], & Thomas C. Boothby[a*]
a) Department of Molecular Biology, University of Wyoming. Laramie, WY 82071
b) Department of Chemistry, University of Wyoming. Laramie, WY 82071
* To whom correspondence should be addressed: tboothby@uwyo.edu

Abstract

Water is essential for metabolism and all life processes. Despite this, a number of organisms distributed across the kingdoms of life can survive near-complete desiccation or anhydrobiosis (life without water). Increases in intracellular viscosity, leading to the formation of a vitrified (glassy) state is necessary, but not sufficient, for conferring desiccation tolerance. What properties of a vitrified system make it desiccation-tolerant or -sensitive are unknown. We have analyzed 18 different *in vitro* vitrified systems, composed of one of three protective disaccharides (trehalose, sucrose, or maltose) and varying amounts of glycerol, quantifying their protective capacity and their material properties in a dry state. We find that protection conferred by mixtures containing maltose correlates strongly with increased water content, increased glass-transition temperature, and reduced glass former fragility, while the protection of glasses formed with sucrose correlates with increased glass transition temperature and the protection conferred by trehalose glasses correlates with reduced glass former fragility. Thus, *in vitro* different vitrified sugars confer protection through distinct material properties. Extending on this, we have examined the material properties of a dry desiccation tolerant and intolerant life stage from four different organisms. In all cases, the dried desiccation tolerant life stage of an organism had an increased glass transition temperature relative to its dried desiccation intolerant life stage, and this trend is seen in three of four organisms when considering reduced glass fragility. These results suggest that while drying of different protective sugars *in vitro* results in vitrified systems with distinct material properties that correlate with their protective capacity, in nature organismal desiccation tolerance relies on a combination of these properties. This study advances our understanding of how protective and non-protective glasses differ in terms of material properties that promote anhydrobiosis. This knowledge presents avenues to develop novel stabilization technologies for pharmaceuticals that currently rely on the cold-chain.

Statement of significance

For the past three decades the anhydrobiosis field has lived with a paradox, while vitrification is necessary for desiccation tolerance it is not sufficient. Understanding what property(s) distinguishes a desiccation tolerant from an intolerant vitrified system and how anhydrobiotic organisms survive drying is one of the enduring mysteries of organismal physiology. Here we show *in vitro* the protective capacity of different vitrifying sugars can be correlated with distinct material properties. However, *in vivo*, diverse desiccation tolerant organisms appear to combine these material properties to promote their survival in a dry state.

Keywords
Vitrification, glass fragility, glass transition temperature, desiccation tolerance, anhydrobiosis, maltose, sucrose, trehalose, water retention.

Highlights

- The protective capacities of different glass forming sugars correlate with distinct material properties.
- Material properties of dried anhydrobiotic organisms differ dramatically when examined in desiccation tolerant and intolerant life stages.

- Organismal desiccation tolerance appears to rely on a combination of properties of the vitrified state including increased glass transition temperature and reduced glass former fragility.

Introduction

Water is required for metabolism and so is often considered essential for life. However, a number of organisms, spread across every biological kingdom, are capable of surviving near-complete water loss through a process known as anhydrobiosis (Greek for "life without water") (1). As organisms dry, they face a number of physical and chemical changes to their cellular environment (1, 2). As water is lost, cellular constituents are concentrated, molecular crowding increases, pH and ionic concentrations change, and osmotic pressure increases (2). These physiochemical changes lead to detrimental perturbations such as protein unfolding, aggregation, and membrane leakage (2). Importantly, drying is not an all-or-nothing process and these changes as well as the perturbation they induce, occur along a continuum, with some perturbations occurring earlier as an organism is dehydrating while others manifest later, once more substantial amounts of water have been lost (1–4). How organisms survive desiccation is one of the enduring mysteries of organismal physiology.

Historically, anhydrobiosis has been thought to be mediated, at least in part, through the concentration of cellular constituents until these constituents solidify into a vitrified material (a glass). In this hypothesis, known as the 'vitrification hypothesis,' glasses slow physical and biochemical change, making them natural promoters of desiccation tolerance. Within the anhydrobiosis field, vitrification is considered a necessary process for desiccation tolerance (5–8).

However, a major shortcoming of the vitrification hypothesis has been known for decades, namely the observation that essentially every biological, or sufficiently heterogeneous, system will vitrify when dried, regardless of whether it is desiccation-tolerant or -sensitive (1, 5–7). This observation implies that while vitrification is necessary, it is not sufficient for desiccation tolerance and that there must be some property, or properties, that distinguishes a protective from a non-protective vitrified state (5, 9). The properties distinguishing a desiccation-protective glass from a non-protective glass are not currently fully understood.

Previous studies have identified that small additions of glycerol changes the protective capacity of trehalose (10). However, the material properties of these mixtures and how they correspond with changes in the level of protection have not been investigated. To address this gap in knowledge, we test the hypothesis that the protective capacity of disaccharide-glycerol mixtures during desiccation correlates with their material properties. These properties include water content, glass transition temperature, and glass former fragility.

Water content is a property of vitrified materials that has been implicated in survival during extreme desiccation (4, 11, 12). Water content refers to the mass percent of water in a desiccated sample. This can be measured by taking the starting mass of a desiccated sample and dividing by the mass of the sample after heating to a temperature sufficient to evaporate residual water. While hydrated, water molecules within a cell are able to solvate and then stabilize sensitive intracellular components. By retaining more water, it has been proposed that a vitrified material could prevent damage to sensitive intracellular components by maintaining hydration shells around them (3, 4).

Glass transition temperature (T_g) is the temperature at which a vitrified solid transitions from a glassy to a rubbery state (13–15). Increases or decreases to the T_g of a vitrified material occur through the inclusion of an additive (16). Increasing the glass transition temperature of a vitrified material has been observed to increase the shelf-life of sensitive proteins in a dry state (17) and is implicated in being essential for survival during desiccation at low relative humidity (3). At the organismal level, it has been demonstrated that many anhydrobiotic organisms survive heating up to, but not beyond, their T_g (6, 18). This suggests that anhydrobiotic organisms rely on being in a vitrified state and the production of small molecules which increase T_g may be an effective strategy for increasing desiccation tolerance.

Finally, glass former fragility has been implicated as a key property of vitrified materials that promotes desiccation tolerance (9). This property distinguishes strong glass forming materials, whose

viscosity increases steadily well before the liquid-to-solid transition, from fragile glass forming materials, whose viscosity increases slowly at first but then rises abruptly at the onset of vitrification (9, 13, 19). It should be noted that in this context, glass fragility/strength does not refer to the brittleness of a vitrified material, but rather to how the viscosity of the material changes as it approaches the point of vitrification. It is hypothesized that strong glass forming materials confer more protection during desiccation than their more fragile counterparts (4, 9, 13, 19). This hypothesis relies on the logic that a fragile glass forming material will not produce a sufficiently viscous state to slow down or prevent perturbation such as protein unfolding and aggregation until it is too late. Conversely, a strong glass forming material will increase in viscosity and provide protection along the continuum of drying.

To empirically test which of these three material properties correlate with desiccation tolerance, we first used a panel of simple reductive systems, each composed of two mediators of desiccation tolerance - a disaccharide including maltose (20, 21), sucrose (1, 5, 22), or trehalose (6, 7, 18, 23–25) and the polyol glycerol (26–28). Comparing the measured material properties (water content, T_g, and glass former fragility) of our disaccharide-glycerol glasses with their *in vitro* protective capacities (Fig. 1a), we find that there is not a strict pattern in terms of the correlation of material properties to protection that all disaccharide follow. Instead, it appears that each disaccharide has a particular material property that is best correlated with its protective capacity.

We extend this analysis into four organismal systems, each of which has a well-characterized desiccation tolerant and intolerant life stage. We find that while the protective capacity of our *in vitro* systems tend to correlate with a single material property, our *in vivo* studies showed a correlation with both increased glass transition temperature and reduced glass fragility to organismal desiccation tolerance. This suggests that anhydrobiotic organisms, spanning different kingdoms of life, modulate multiple material properties to promote organismal desiccation tolerance.

The extension of our mechanistic understanding of the principles underlying desiccation-tolerance provide insights into how organisms can cope with changing, often extreme, environments. These findings also help to address the decades long paradox that some glasses are protective, and others not, during desiccation, by providing insights into material properties that promote the protective capacity of different vitrifying mixtures. Our work identifies increased glass transition temperature and glass fragility as major considerations in the development of technologies for the dry preservation of pharmaceuticals and the engineering of crops that are better able to withstand climate change and extreme weather.

Materials and Methods

Disaccharide-glycerol mixtures

D-Maltose monohydrate was sourced from Caisson Labs (M004-500GM). D-Sucrose was sourced from Sigma-Aldrich (S0389-500G). D-Trehalose dihydrate was sourced from VWR (VWRB3599-1KG). Glycerol was sourced from Biobasic (GB0232). Mixtures of each disaccharide and glycerol were made in 25 mM Tris at pH 7.0. Individual masses of each component were formulated (weight by weight) to additively produce mixtures of 10 g/L.

Sample Desiccation

Samples were desiccated using a speedvac (Savant SpeedVac SC110 with a Thermo OFP400 vacuum pump) for 16 hours. Prior to desiccation, 1 mL aliquot samples were dispensed into individual plastic weigh-boats (for aqueous samples) and at least 200 mg of organism samples were similarly loaded into individual plastic weigh-boats. The greater surface area of the weigh-boat, as opposed to Eppendorf tubes, allows for even desiccation of the entire sample, which reduces noise on the DSC. After the 16 hour desiccation, DSC samples were transferred to pre-massed pairs of DSC aluminum hermetic pan and aluminum hermetic lids (TA 900793.901 and 901684.901, respectively) while TGA samples were transferred to pre-tared platinum crucibles (TA 957207.904), and XRD samples were kept in the

desiccation weighboats. DSC sample masses were determined after the sample was sealed within the pan and lid.

Single crystal X-ray diffractometry

Powder diffraction patterns for the samples were measured at 20 °C on a Bruker SMART APEX II CCD area detector system equipped with a graphite monochromator and a Mo K fine-focus sealed tube operated at 1.2 kW power. The dried samples were rolled into a ball of approximate diameter 0.5 mm, mounted on a goniometer head using a glass fiber, and centered using the APEX2 software. The detector was placed at 6.12 cm during the data collection. Four frames of data were collected at four different sets of angles with a scan width of 0.2 ° and an exposure time of 3 min per frame. The frames were integrated using the APEX2 program. The measured powder diffraction images were integrated, and the data were plotted in the 5 to 50 ° 2θ. All analysis was performed using the APEX3 Software Suite V2017.3-0, Bruker AXS Inc.: Madison, WI, 2017.

Lactate dehydrogenase (LDH) enzyme protection assay

LDH assays were performed using a combination of methodologies described in Goyal *et al.*, 2005 and Boothby *et al.*, 2017. Briefly, stock solutions of 25 mM Tris HCl (pH 7.0), 100 mM sodium phosphate (pH 6.0), 2 mM pyruvate, and 10 mM NADH were prepared in bulk and stored at room temperature prior to assay. L-Lactate Dehydrogenase (LDH) was sourced from Sigma (SKU #10127230001) and is supplied in ammonium sulfate at a pH of approximately 7. Prior to assay, LDH was diluted to a working concentration of 1 g/L. Experimental disaccharide-glycerol mixtures were formulated with LDH at a 1:10 (LDH:disaccharide-glycerol) ratio. Enough solution was prepared for three test excipient replicates and three control replicates each with a total volume of 50 μL. Each experimental and control mixture were aliquoted into a 1.5 mL microcentrifuge tube. The test mixtures were then vacuum desiccated for 16 hours with controls kept refrigerated at 4 °C. After vacuum desiccation, control and test excipient mixtures were brought to 250 μL total volume. Absorbance readings at 340 nm wavelength were taken every two seconds for 60 seconds with a quartz cuvette on a Thermo Scientific NanoDrop One[c] (Thermo Scientific 840274200) spectrophotometer. A 100mM sodium phosphate and 2mM pyruvate solution was used as a blank. For control samples and experimental samples, 10 μL of control mixture or 10 μL of experimental sample mixture were combined with 10 μL of NADH and 980 μL of the 100mM sodium phosphate, 2mM pyruvate solution and then were measured.

This same procedure is used to measure the A340 of the experimental mixtures. A ratio of experimental over control, multiplied by one hundred, will produce the percent protection of the experimental mixture. All raw LDH protection data as well as calculation of percent protection is available in Supplemental File 1.

Thermogravimetric analysis

Samples were run on a TA TGA5500 instrument in 100 μL platinum crucibles (TA 952018.906). Crucibles were tared prior to each run and prior to sample loading. Crucibles were loaded with between 5 mg and 10 mg of sample mixture. Each sample was heated from 30 °C to 220 °C at a 10 °C per minute ramp. All TGA measurements are available in Supplemental File 2 and Supplemental File 3.

Differential scanning calorimetry

Samples were run on a TA DSC2500 instrument with Trios software (TA Instruments TRIOS version #5.0.0.44608). Analysis of DSC output was performed using Trios software. The heating run consisted of being equilibrated at -10 °C and then heated using a 10 °C per minute ramp to 220 °C. All raw DSC measurements are available in Supplemental File 4 and Supplemental File 5.

Fragility (m-index) calculation

Trios software (TA Instruments TRIOS version #5.0.0.44608) provided by TA Instruments was used to perform analysis of the DSC data. Calculations of glass fragility (m-index) were performed based on equation 14 proposed by Crowley and Zografi (29). On a thermogram with a completed heating ramp to 220 °C, the degradation peak, melt peak, and glass transition were identified. The Trios software built-in Onset and Endset analysis was used to determine the Glass transition onset and offset (endset). The software-identified glass transition onset and offset was used to calculate the m-index using Crowley and Zografi's equation 14 (29), and a mean of each set of replicates was obtained. All fragility calculations are available in Supplemental File 6.

Selected organisms for in vivo *assays*

Arabidopsis thaliana, Artemia franciscana, Caenorhabditis elegans, and *Saccharomyces cerevisiae* were all selected based on availability of access to both desiccation sensitive and desiccation tolerant life stages.

Arabidopsis thaliana seeds were acquired from Carolina Biological Supply Company (#177600) and adult plants were grown at 22 °C with a 12 hour light and 12 hour dark cycle.

Artemia franciscana adults (#1) and cysts (#11) were acquired from the Northeast Brine Shrimp, LLC. *A. franciscana* adults were separated from culture media by tube-top filtration using a pluriSelect 200 μm pluriStrainer (#43-50200-03) prior to desiccation.

Caenorhabditis elegans non-dauered daf-2 strains were cultured in S Medium (30) at 16 °C and fed with *E. coli* OP50. Dauered and dauered pre-conditioned daf-2 strain worms were cultured identically to non-dauered worms but when the initial aliquot of *E. coli* OP50 were consumed an additional five days of incubation at 25 °C was given to starve the culture and induce dauer arrest. Pre-conditioned dauer worms were additionally placed on non-spotted agar plates in a 95% relative humidity atmosphere for 3 additional days. All three *C. elegans* sample sets were separated from media and residual OP50 food stock by tube-top filtration using a pluriSelect 200 μm pluriStrainer (#43-50200-03) prior to desiccation.

Saccharomyces cerevisiae strain BY4742 were cultured aerobically in YPD media (31) at 30 °C. After nine hours samples were taken representing the logarithmic growth stage yeast. The remaining culture was allowed to grow for an additional five days to ensure confluent growth in the stationary phase. Both logarithmic and stationary phase samples were pelleted by centrifugation, media decanted and a water wash of cell pellets was performed prior to desiccation.

Statistical methods:

All statistical methods are calculated using a Student's T-Test with a p-value of less than 0.05 being one level of statistical significance (*), less than 0.01 being two levels of statistical significance (**), and less than 0.001 being three levels of statistical significance (***). All error values represent 95% confidence intervals.

Results

Disaccharide-glycerol mixtures vitrify when dried.

To begin to address which material properties correlate with protective capacity in a vitreous state, we generated 18 different glass forming mixtures composed of one of three disaccharides (maltose, sucrose, or trehalose) and varying amounts of glycerol (10, 32). Previous studies have identified that small additions of glycerol changes the protective capacity of trehalose. However, the material properties of these mixtures and how they correlate with changes in the level of protection have not been investigated.

Furthermore, it is not known to what extent additions of glycerol will influence the material and protective properties of other disaccharides or how these two properties are linked (10).

Maltose is a reducing disaccharide consisting of two glucose molecules joined by an α (1→4) bond (33). Sucrose is a non-reducing disaccharide formed by the glycosidic linkage between C1 of a glucose molecule to the C2 of a fructose molecule (34). Trehalose is a non-reducing disaccharide formed through the (1-1) glycosidic linkage of two glucose molecules (35). All three of these disaccharides are known to accumulate in a number of anhydrobiotic organisms during drying and in many cases they are known to be essential for surviving desiccation (6, 18, 20, 21, 23–25). Glycerol is a polyol that has been implicated in the tolerance of several stresses ranging from drying to freezing (26, 28).

Mixtures containing 100%, 97.5%, 95%, 92.5%, 90%, and 87.5% of a single disaccharide (maltose, sucrose, or trehalose), combined with glycerol (weight % by weight % with glycerol) were created. These percentages were selected to allow for comparison with trehalose-glycerol material measurements from previous studies generated through different methods (10). Mixtures were dried overnight in a vacuum desiccator for 16 hours to produce glasses.

To ensure that these mixtures vitrified, rather than crystallized, each sample's powder diffraction pattern was observed by powder X-ray diffraction (XRD) using Mo Kα radiation. The integrated plots of our 18 vitrifying samples contain a nearly identical broad absorption, and do not reveal any sharp peaks (Fig. S1a and S1b). The absence of sharp peaks indicates that the samples are glassy with no crystallinity (36, 37). Powder diffraction data was also measured for a desiccated sample of D-(+)-glucose, which is known to crystalize when dried. In contrast to the XRD patterns measured for the disaccharide-glycerol samples, the diffraction pattern for glucose exhibited a large number of distinct, closely spaced peaks due to the crystalline nature of this sample (Fig. S1a and S1b). These results indicate that maltose, sucrose, or trehalose by themselves or in conjunction with varying degrees of glycerol vitrify when dried.

Disaccharide-glycerol mixtures have varying levels of protection during desiccation.

To address the question of which property(s) of a vitrified solid correlate with protective capacity during desiccation, we assessed the ability of our 18 disaccharide-glycerol mixtures to protect the enzyme lactate dehydrogenase (LDH) during desiccation (7, 38, 39) (Fig. 1b). Previous reports have shown that LDH is sensitive to desiccation and that drying and rehydration of this enzyme results in ~95-99% loss in functionality (39) (Fig. 1b).

Taking the ratio of the enzymatic activity of rehydrated *versus* control LDH, we observed that the protection of desiccated LDH varied significantly between different disaccharide-glycerol mixtures (Fig. 1c).

For maltose-glycerol mixtures, the highest level of protection was observed for our 100% maltose sample, while the lowest level of protection was conferred by the 87.5% maltose sample. No significant difference in protection was observed until the percentage of maltose in mixtures reached 92.5%, after which protection steadily decreased (Fig. 1c, top panel).

Similar to maltose-glycerol mixtures, sucrose-glycerol mixtures showed the highest level of protection at 100% sucrose, while the lowest level of protection was conferred by the 87.5% sucrose sample. However, unlike maltose samples, sucrose mixtures rapidly lost protective capacity with statistically significant decreases in protection being observed upon the first (2.5%) addition of glycerol (Fig. 1b, middle panel).

Trehalose-glycerol mixtures differed from both maltose and sucrose mixtures in that the highest level of protection was achieved at 97.5% (Fig. 1c, bottom panel). Additionally, while mixing of maltose or sucrose with glycerol resulted in decreases in protection, additions of glycerol to trehalose were found to have a nonmonotonic relationship with protection (Fig. 1c, bottom panel).

These results demonstrate that different disaccharide and glycerol mixtures provide varying levels of protection to LDH during desiccation and rehydration, with trehalose responding in a non-monotonic fashion, maltose decreasing in protective capacity in a linear fashion, and protection conferred by sucrose decreasing exponentially.

Water content correlates with the protective capacity of maltose-glycerol, but not trehalose-glycerol or sucrose-glycerol, mixtures.

To begin to assess which properties of a system correlate with protection, we first assessed whether or not water content could account for these differences. In the field of desiccation tolerance, it has been proposed that desiccation tolerant organisms may be able to retain more water than their desiccation sensitive counterparts. An increase in water content would help increase the proportion of proteome, membranes, and other vital cellular components that remain solvated. The increased quantity of retained water in a desiccated state has been proposed in a number of mechanisms including the water replacement, water caging, and preferential exclusion theories *(4). To assess whether the differences in protection observed in our vitrified samples correspond to the amount of water they retain, we tested each of our mixtures using thermogravimetric analysis (TGA) (Fig. 2a). Water contents of our 18 dry mixtures ranged from 6.98 to 0.84% (Fig. 2b). Pure dry trehalose and sucrose contained approximately the same amount of retained water (5-6%), while pure dry maltose retained significantly less water (~1%) (Fig. 2b). In maltose-glycerol mixtures the amount of retained water increased with each addition of glycerol (Fig. 2b). In contrast, water content did not vary in any sucrose-glycerol mixture or trehalose-glycerol mixture, relative to pure samples (Fig. 2b).*

After observing distinct water retentive behaviors in dry disaccharide-glycerol mixtures, we assessed the relationship between water content and protection. For maltose mixtures, this correlative analysis produced an R^2 value of 0.973 (Fig. 2c), an R^2 value of 0.131 for sucrose mixtures (Fig. 2d), and R^2 value of 0.204 for trehalose mixtures (Fig. 2e). These results indicate that for maltose-glycerol systems the amount of retained water is a good indicator of the protective capacity in the dry state. However, the amount of water in mixtures made of dry trehalose or sucrose and glycerol is a poor indicator of protective capacity (Fig. 2f).

An increase in the glass transition temperature correlates with protection conferred by maltose-glycerol and to a lesser extend sucrose-glycerol, but not trehalose-glycerol mixtures in the dry state.

After observing that water retention is a poor indicator of the protective capacity of trehalose- and sucrose-glycerol glasses, we wondered if glass transition temperature (T_g) might be a property that correlates with the stabilizing effects of these sugars. Glass transition temperature (T_g) is the temperature at which a hard glassy material will begin to transition into a rubbery solid (40). Figure 3a is a schematic illustration of how increases or decreases in the T_g are captured and visualized on a thermogram. Previous work has established that even small amounts of additives, such as glycerol, can lead to decreased or increased T_g of a vitrifying material (Fig. 3a) (41–46). With this in mind, we were curious if different additions of glycerol to our disaccharides would serve to increase or decrease the T_g resulting glasses, and whether or not these changes in T_g correlates with the protective capacity of our mixtures.

The glass transition temperature onset and offset, the temperatures that the material starts and stops undergoing a change from a glassy state to a rubbery state, were assessed using differential scanning calorimetry (DSC), and the glass transition midpoint temperature calculated by taking the mean of the onset and offset temperature (Supplemental File 6). Figures 3b, S3a, and S3b show the average T_g onset, offset, and midpoint for each of our mixtures. Here one can see that when considering the glass transition midpoint even small additions of glycerol, starting at 2.5%, act to decrease the T_g for both maltose and trehalose, while decreasing the T_g of sucrose is only observed with a larger (12.5%) addition of glycerol (Fig. 3b). Interestingly, glycerol acts to both increase and decrease the T_g of trehalose and this effect is observed to be non-monotonic (Fig. 3c).

However, when considering the onset or offset glass transition temperature for each set of disaccharide-glycerol mixtures, we saw different behaviors appear. For example, when observing changes to the glass transition onset temperature for the maltose-glycerol mixtures, only after the addition of 10% glycerol did the glass transition onset temperature decrease significantly (Fig. S3a). Similarly, sucrose did not significantly change until after the addition of 7.5% glycerol and even then only demonstrated

statistically significant decreases in the glass transition onset temperature (Fig. S3a). Only the trehalose-glycerol mixtures show statistically significant changes in the glass transition onset temperature with the first addition of glycerol (Fig. S3a). The trehalose-glycerol mixtures also continued to show statistically significant decreases in glass transition onset temperature for all additional glycerol additions measured (Fig. S3a).

When observing the offset of glass transition temperature for each of the disaccharide-glycerol mixtures, we observed that the maltose-glycerol and sucrose-glycerol mixtures demonstrated similar behavior to the midpoint observations. Specifically, starting at 2.5% for trehalose and 5% for maltose, glycerol acts to decrease the glass transition offset temperature (Fig. S3b). On the other hand, sucrose does not show a statistically significant change in the glass transition offset until after the addition of 5% glycerol where it has increased the offset temperature and again after the addition of 12.5% glycerol where it has decreased the offset temperature (Fig. S3b).

Next, we evaluated the relationship between protective capacity and the onset, offset, and midpoint T_g for each mixture (Fig. 3d, 3e, 3f, 3g and S4a). This correlative analysis produced positive correlations with R^2 values ranging from 0.978 to 0.906 for maltose (Fig. 3d and S4a) and positive correlations with R^2 values ranging from 0.377 to 0.100 for sucrose (Fig. 3e). For trehalose the R^2 values ranged from 0.395 to 0.002 but the correlations were negative, negative, and positive for the onset, midpoint, and offset glass transition temperatures respectively (Fig. 3f and S4a). We observe that the protective capacity of the maltose-glycerol mixtures are significantly influenced by variation in their T_g, that the protective capacity of the sucrose-glycerol mixtures are moderately influenced by variation in their T_g, and that there appears to be little relationship between variation in the T_g and protective capacity for the trehalose-glycerol mixtures (Fig. 3g).

Our results demonstrate that generally, protection positively correlates with increasing T_g. However, this correlation is clearly stronger for some sugar-glasses (e.g., maltose) compared to others (e.g., sucrose).

Vitrified maltose-glycerol and trehalose-glycerol mixtures demonstrate a reduction in glass former fragility that is correlated with protection.

Next, we empirically determined the glass former fragility of our disaccharide-glycerol mixtures (Fig. 4a). Historically, the fragility of a glass forming mixture has been represented as an m-index, where increasing fragility is represented by increasing m-index values (15, 29). Previous work has confirmed that varying trehalose-glycerol content results in mixtures with different glass former fragilities in a non-monotonic fashion (10).

Glass fragility (m-index), was calculated from DSC thermogram outputs using established methods (Fig. 4a) (29). The fragility of glass forming solutions composed from pure disaccharides was lowest for maltose, followed by trehalose, and finally sucrose (Fig. 4b). For maltose samples, fragility steadily increased with each addition of glycerol (Fig. 4b), however for both sucrose and trehalose small additions of glycerol (up to 5 and 2.5%, respectively) decreased fragility (Fig. 4b). However, greater additions of glycerol to both trehalose and sucrose increased fragility (Fig. 4b).

Next, we also assessed the relationship between the fragility of our glass forming mixtures and protection of LDH. This correlative analysis produced an R^2 value of 0.969 for maltose (Fig. 4c), an R^2 value of 0.032 for sucrose (Fig. 4d), and R^2 value of 0.678 for trehalose (Fig. 4e). This indicates that for maltose, and to a lesser extent trehalose, observed variation in glass former fragility can explain the protective capacity of the desiccated mixtures (Fig. 4f). Again, just as with water retention and shifts in the T_g, we see that the addition of glycerol induces different degrees of glass former fragility and that this property is a good indicator of protection for some sugar glasses, but not for others.

Increased T_g *and decreased glass former fragility are characteristics of anhydrobiotic organisms.*

We wondered if the correlation between material properties (such as minimal glass fragility or anti-plasticization) observed *in vitro* to correlate with protection also correlated with survival during *in vivo* desiccation. Here we considered reduced glass fragility and anti-plasticization, but not water retention,

since water content has previously been observed to influence glass-like properties (16, 47–49). This influence is observed in our samples, where for example in maltose-glycerol mixtures, we see a very strong correlation ($R^2 = 0.989$) between water content and increased *Tg* (Fig. S2a).

We measured the T_g and m-indexes of four desiccation tolerant organisms when in a desiccation sensitive life stage or a desiccation tolerant life stage. The four desiccation tolerant organisms we selected for this study were: the plant *Arabidopsis thaliana*, the brine shrimp *Artemia franciscana*, the nematode worm *Caenorhabditis elegans*, and yeast *Saccharomyces cerevisiae* (Fig. 5a).

Each of these selected organisms utilizes a variety of mediators to achieve desiccation tolerance. For example, *A. thaliana* seeds effectively stockpile sucrose and oligosaccharides when reaching a mature and desiccated state (50), *A. franciscana* cysts (51), *C. elegans* dauer larva (26, 51, 52), and *S. cerevisiae* accumulate trehalose (24, 53). Additionally, *A. franciscana* cysts accumulate glycerol in a desiccated state (51), and stationary phase *S. cerevisiae* convert glycerol to trehalose (24, 53).

For *A. thaliana*, we saw that there was a significant increase in T_g midpoint when comparing dry leaf material (desiccation sensitive life stage) and seed (desiccation tolerant life stage) (Fig. 5b). Likewise, for *A. franciscana*, there was a significant increase in T_g midpoint between the adult (desiccation sensitive life stage) and cyst (desiccation tolerant life stage) (Fig. 5b). For *C. elegans*, this trend continued with a significant increase in T_g midpoint being observed between non-dauered worms (desiccation sensitive life stage) and dauered worms (desiccation sensitive intermediate life stage) as well as a further significant increase in T_g midpoint between the non-dauered worm and dauered preconditioned worm (desiccation tolerant life stage) (Fig. 5b). And finally, for *S. cerevisiae*, we saw a statistical increase between the exponential phase (desiccation sensitive life stage) and stationary phase (desiccation tolerant life stage) when measuring T_g midpoint (Fig. 5b).

Thus, for all four of the desiccation tolerant organisms tested we observe significantly increased T_g in the anhydrobiotic state, indicating that increased T_g correlates with survival during drying.

Next, we evaluated our four selected organisms 'life stages for changes in m-index (glass former fragility). For *A. thaliana*, we saw that there was a significant decrease between the leaf (desiccation sensitive life stage) and seed (desiccation tolerant life stage) when measuring m-index (Fig. 5c). For *A. franciscana*, we saw no statistical difference between the adult (desiccation sensitive life stage) and cyst (desiccation tolerant life stage) when measuring m-index (Fig. 5c). For *C. elegans*, we saw no significant difference between the non-dauered worm (desiccation sensitive life stage) and dauered worm (desiccation sensitive intermediate life stage) but a significant decrease between the non-dauered worm and dauered preconditioned worm (desiccation tolerant life stage) when measuring m-index (Fig. 5c). For *S. cerevisiae*, we saw a significant decrease between the exponential phase (desiccation sensitive life stage) and stationary phase (desiccation tolerant life stage) when measuring m-index (Fig. 5c).

Taken together, these results indicate that while *in vitro* simple mixtures of protectants vary widely in what properties correlate with protection in the vitrified state, *in vivo* both increased glass transition temperature and decreased fragility are good indicators of survival in the dry state.

Discussion and conclusions

Since its conception, the vitrification hypothesis has provided a compelling possible explanation as to how anhydrobiotic organisms preserve their cells and cellular components during desiccation (1, 5–7). However, while vitrification is considered necessary for desiccation tolerance it is not sufficient (5, 9). This implies that there is some property of a glassy material that makes it more or less protective.

Here we have quantified the protective capacity and material properties of 18 different vitrified systems, each composed of one of three different disaccharides (maltose, sucrose, and trehalose) formulated with varying amounts of glycerol (0-12.5%). We find that both protective capacity and material properties of disaccharide-glycerol mixtures are modulated differently depending on the disaccharide used. Consistent with this, water retention (maltose), increased T_g (sucrose), and reduced glass fragility (trehalose) each correlated best with protection for a particular disaccharide. Interestingly, reduced fragility and increased glass transition (anti-plasticization) is observed in desiccation-tolerant life

stages of diverse organisms. Thus, individual protective properties observed for reductive systems appear to be used in combination *in vivo*.

Water retention and its effects on glass transition temperature and glass former fragility.

Our results demonstrate that different disaccharide-glycerol mixtures retain different quantities of water. Furthermore, the relationship between retained water and protection also varies between disaccharide-glycerol mixtures. Maltose-glycerol mixtures display a significant positive correlation between water retention and enzyme protection, while the sucrose-glycerol and trehalose-glycerol mixtures show only mildly positive correlations (R^2 =0.131 and .204, respectively).

This is of interest, as water has traditionally been considered the most important plasticizing agent of biological and hydrophilic materials, meaning that increasing water content in a vitrified material typically leads to a decrease in T_g, which is also considered to reduce protection. However, while this is generally true, there have been reports of *bona fide* antiplasticization effects of water (48). Here we observe that water content of maltose-, sucrose-, and trehalose-glycerol glasses largely does not have a strong plasticizing effect. The only negative correlation between water content and decreased T_g was observed for the sucrose-glycerol mixtures (R^2 = 0.44, Fig. S2c). In trehalose-glycerol mixtures, there was essentially no correlation between water content and decreased T_g (R^2 = 0.004, Fig. S2e). Finally, in maltose-glycerol mixtures, rather than seeing water correlate with decreased T_g, surprisingly we observe a strong correlation between water content and increased T_g (R^2 = 0.989, Fig. S2a). This again showcases how each of the disaccharides, when in a desiccated disaccharide-glycerol mixture, displays disparate changes in material properties.

When instead considering the relationship between water content and glass fragility, we again observe differing results by disaccharide-glycerol mixture. Here we see that the desiccated maltose-glycerol mixtures have a statistically significant relationship (R^2 = 0.928, Fig. S2b), sucrose has a strong relationship (R^2 = 0.882, Fig. S2d), and trehalose has a very weak relationship at (R^2 = 0.204, Fig. S2f).

These results might lead one to believe that at the water contents examined here (< 8%) water retention might be a potential predictor of enzyme protective capacity. However, water content also seems to influence other material properties of the vitrified system in a non-stereotyped fashion. For example, increasing water content in maltose-glycerol mixtures strongly correlates with reduced glass fragility, while in sucrose and trehalose-glycerol mixtures increasing water content increases fragility. Thus, we conclude that water content itself is not a good predictor of desiccation tolerance nor of other properties of a vitrified system.

The protective capacity of sucrose-glycerol mixtures was most influenced by increases and decreases in glass transition temperature.

The relationship of increases or decreases in T_g with protection varied between different disaccharide-glycerol mixtures, but was most important for the sucrose-glycerol mixtures. While we observed that only maltose-glycerol mixtures had a strong relationship between increased T_g and protection (Fig. 3d), in the sucrose-glycerol mixtures we see that addition of glycerol results in an increase in the T_g when added up to 5% , but then further addition of glycerol causes a significant decrease in the T_g. Furthermore, the influence of glycerol on the T_g of sucrose-glycerol mixtures correlates moderately with protection, but is the highest correlation with respect to protective capacity. Finally, the trehalose-glycerol mixtures we see no significant variation in the glass transition midpoint until the addition of 12.25% glycerol where it decreases the T_g, and the small changes in T_g that are observed show no correlation with protection.

Thus while increases in T_g are predictive of the protection conferred by maltose-glycerol mixtures, and to a lesser extent sucrose-glycerol, this predictive capacity does not extend to all vitrified systems.

Offset glass transition temperature appears to capture the relationship between desiccation survival and material property better than glass transition onset or midpoint

When referring to the glass transition or the material properties based on the glass transition, the standard measure is to use the glass transition midpoint. This value is inherently influenced by both the glass transition onset and offset temperatures (Fig. 3b, S3a, and S3b). The glass transition offset temperature is representative of the point at which the 'glassy' nature of a vitreous system is finally overcome (Fig. S3b). By contrast the glass transition onset is only representative of the start of the transition of a 'glassy' state to a rubber-like solid (Fig. S3a).

In evaluating the relationship between T_g and protection, we observed a dramatic variation in this correlation depending on whether we used the onset, midpoint, or offset glass transition temperature (Fig. S4a). Here we have reported midpoint T_g as is convention, but also have included correlations between protection and onset/offset T_g (Fig. S4a).

Disaccharide-glycerol mixtures with similar concentrations produce fragilities of differing glass former fragility (m-index).

The fragility of different glass former mixtures varied by disaccharide. Only maltose and trehalose showed evidence of a relationship between glass fragility and enzyme protective capacity. Interestingly, when comparing different disaccharide-glycerol systems that provide similar protective capacity, those mixtures did not necessarily produce glasses with similar glass former fragility (m-index) measurements. For example, when comparing the 97.5% maltose, 97.5% sucrose, and 92.5% trehalose disaccharide-glycerol mixtures that provide approximately 30% enzyme protection during desiccation (30.21%, 30.26, and 36.72% respectively), those mixtures produced had a glass former fragility (m-index) of 17.60, 74.0, and 121.62 respectively (Table 1). In addition, when comparing the most protective mixtures for each disaccharide-glycerol mixture, 100% maltose, 100% sucrose and 97.5% trehalose, only maltose and trehalose produced the lowest glass former fragility (m-index) measurement. This indicates that each disaccharide-glycerol system produced glass former fragility patterns that are only comparable within that system and not between different disaccharide-glycerol systems.

Both change in T_g *and glass former fragility are well correlated with desiccation tolerant organism life stage.*

The results from our *in vitro* experiments, while novel on their own, beg the question of whether these findings apply to whole desiccation tolerant organisms. Examining four different organisms in both a desiccation-tolerant and -sensitive life stage we observe that both increased T_g and reduced m-index (glass fragility) are hallmarks of successful anhydrobiosis. Specifically, when considering changes in T_g, we see that for each organism, *A. thaliana*, *A. franciscana*, *C. elegans*, and *S. cerevisiae*, there is a statistically significant increase in T_g when comparing the desiccation-sensitive life stage to the desiccation-tolerant life stage. When considering the impact of glass former fragility, *A. thaliana*, *C. elegans*, and *S. cerevisiae* all demonstrate a statistical decrease in glass former fragility when comparing the desiccation-sensitive life stage to the desiccation-tolerant life stage. In fact, only *A. franciscana* did not demonstrate a statistically significant decrease in glass former fragility when comparing the desiccation-sensitive (adult) life stage to the desiccation-tolerant (cyst) life stage.

Figure 6 provides an overview of what we envision is occurring to enable changes in the T_g (Fig. 6a) and glass former fragility (Fig. 6b and 6c) to be protective during desiccation. In Figure 6a we depict a glass with a decreased T_g as one with relatively few and/or weak bonds, which do not effectively slow down molecular motions leading to the destabilization and/or aggregation of embedded clients over time. In contrast, a glass with an increased T_g is one with increased and/or stronger bonds leading to reduction in molecular motion and an increase in stability of a client over time.

Figure 6b illustrates what we envision is happening when a glass forming mixture forms a weak glass. As water is lost, the weak glass forming ability of the mixture does not become viscous (green) soon enough to prevent drying induced damage (tan). Specifically, a weak glass former material will only

begin gaining sufficient viscosity to confer protection after significant water loss. Conversely, Figure 6c illustrates how a strong glass forming mixture starts to gain viscosity (purple) much earlier in the desiccation process compared to weaker glass forming materials. This steady increase in viscosity, allows for the slowing detrimental perturbations (tan) that manifest early during drying.

While previous studies have examined the glass former fragility of seeds in relationship to their desiccation tolerance, to our knowledge this is the first study examining changes in T_g and glass former fragility in animal and fungal systems (3, 9, 54–57). These comparative organismal studies show a stark contrast to our *in vitro* data, in that rather than a single material property correlating with protection, it appears that in living anhydrobiotic systems both increased T_g and reduced fragility correlate with survival. This may be due the nature of the *in vitro* systems being simple, or less complex, in their interactions while the *in vivo* studies are by their nature much more complex, both in their material makeup and interactions.

These results hint at the fact that living systems likely make use of multiple mediators of desiccation tolerance to produce protective glasses. Indeed, an emerging paradigm in the anhydrobiosis field is that beyond disaccharides, other molecules, such as intrinsically disordered proteins play vital roles in preserving biological function in the solid state.

Our study advances our understanding of what properties of a vitrified system promote desiccation tolerance and the phenomenon of anhydrobiosis both *in vitro* and *in vivo*. A deeper understanding of natural desiccation tolerance promises to provide avenues for pursuing real world applications such as biobanking of seeds and tissues, stabilization of pharmaceuticals, and the generation of stress tolerant crops.

References

1. Crowe, J.H., F.A. Hoekstra, and L.M. Crowe. 1992. Anhydrobiosis. *Annu. Rev. Physiol.* 54:579–599.

2. Hesgrove, C., and T.C. Boothby. 2020. The biology of tardigrade disordered proteins in extreme stress tolerance. *Cell Commun. Signal.* 18:178.

3. Ballesteros, D., H.W. Pritchard, and C. Walters. 2020. Dry architecture: towards the understanding of the variation of longevity in desiccation-tolerant germplasm. *Seed Sci. Res.* 30:142–155.

4. Hibshman, J.D., J.S. Clegg, and B. Goldstein. 2020. Mechanisms of Desiccation Tolerance: Themes and Variations in Brine Shrimp, Roundworms, and Tardigrades. *Front. Physiol.* 11:592016.

5. Crowe, J.H., J.F. Carpenter, and L.M. Crowe. 1998. The role of vitrification in anhydrobiosis. *Annu. Rev. Physiol.* 60:73–103.

6. Sakurai, M., T. Furuki, K.-I. Akao, D. Tanaka, Y. Nakahara, T. Kikawada, M. Watanabe, and T. Okuda. 2008. Vitrification is essential for anhydrobiosis in an African chironomid, Polypedilum vanderplanki. *Proc. Natl. Acad. Sci. U. S. A.* 105:5093–5098.

7. Boothby, T.C., H. Tapia, A.H. Brozena, S. Piszkiewicz, A.E. Smith, I. Giovannini, L. Rebecchi, G.J. Pielak, D. Koshland, and B. Goldstein. 2017. Tardigrades Use Intrinsically Disordered Proteins to Survive Desiccation. *Mol. Cell*. 65:975–984.e5.

8. Boothby, T.C. 2021. Water content influences the vitrified properties of CAHS proteins. *Mol. Cell*. 81:411–413.

9. Ballesteros, D., and C. Walters. 2019. Solid-State Biology and Seed Longevity: A Mechanical Analysis of Glasses in Pea and Soybean Embryonic Axes. *Front. Plant Sci.* 10:920.

10. Weng, L., and G.D. Elliott. 2015. Local minimum in fragility for trehalose/glycerol mixtures: implications for biopharmaceutical stabilization. *J. Phys. Chem. B*. 119:6820–6827.

11. Wright, J.C. 1989. Desiccation tolerance and water-retentive mechanisms in tardigrades. *J. Exp. Biol.* 142:267–292.

12. Hoekstra, F.A., E.A. Golovina, and J. Buitink. 2001. Mechanisms of plant desiccation tolerance. *Trends Plant Sci.* 6:431–438.

13. Angell, C.A. 1995. The old problems of glass and the glass transition, and the many new twists. *Proc. Natl. Acad. Sci. U. S. A.* 92:6675–6682.

14. Angell, C.A. 1997. Entropy, fragility, "landscapes", and the glass transition. In: Complex Behaviour of Glassy Systems. Springer Berlin Heidelberg. pp. 1–21.

15. Ito, K., C.T. Moynihan, and C.A. Angell. 1999. Thermodynamic determination of fragility in liquids and a fragile-to-strong liquid transition in water. *Nature*. 398:492–495.

16. Immergut, E.H., and H.F. Mark. 1965. Principles of Plasticization. In: <bold>Plasticization</bold> and Plasticizer Processes. AMERICAN CHEMICAL SOCIETY. pp. 1–26.

17. Anopchenko, A., T. Psurek, D. VanderHart, J.F. Douglas, and J. Obrzut. 2006. Dielectric study of the antiplasticization of trehalose by glycerol. *Phys. Rev. E Stat. Nonlin. Soft Matter Phys.* 74:031501.

18. Boothby, T.C. 2019. Mechanisms and evolution of resistance to environmental extremes in animals. *Evodevo*. 10:30.

19. Angell, C.A. Entropy, fragility, "landscapes", and the glass transition. *Complex Behaviour of Glassy Systems*. 1–21.

20. Dinakar, C., and D. Bartels. 2013. Desiccation tolerance in resurrection plants: new insights from transcriptome, proteome and metabolome analysis. *Front. Plant Sci.* 4:482.

21. Gechev, T.S., M. Benina, T. Obata, T. Tohge, N. Sujeeth, I. Minkov, J. Hille, M.-R. Temanni, A.S. Marriott, E. Bergström, J. Thomas-Oates, C. Antonio, B. Mueller-Roeber, J.H.M. Schippers, A.R. Fernie, and V. Toneva. 2013. Molecular mechanisms of desiccation tolerance in the resurrection glacial relic Haberlea rhodopensis. *Cell. Mol. Life Sci.* 70:689–709.

22. Crowe, L.M. 2002. Lessons from nature: the role of sugars in anhydrobiosis. *Comp. Biochem. Physiol. A Mol. Integr. Physiol.* 131:505–513.

23. Tapia, H., and D.E. Koshland. 2014. Trehalose is a versatile and long-lived chaperone for desiccation tolerance. *Curr. Biol.* 24:2758–2766.

24. Tapia, H., L. Young, D. Fox, C.R. Bertozzi, and D. Koshland. 2015. Increasing intracellular trehalose is sufficient to confer desiccation tolerance to Saccharomyces cerevisiae. *Proc. Natl. Acad. Sci. U. S. A.* 112:6122–6127.

25. Loomis, S.H., and K.A.C. Madin. 1980. Anhydrobiosis in nematodes: biosynthesis of trehalose. *Journal of Experimental*.

26. Womersley, C., and L. Smith. 1981. Anhydrobiosis in nematodes—I. The role of glycerol myo-inositol and trehalose during desiccation. *Comparative Biochemistry and Physiology Part B: Comparative Biochemistry*. 70:579–586.

27. Womersley, C. 1981. Biochemical and physiological aspects of anhydrobiosis. *Comparative Biochemistry and Physiology Part B: Comparative Biochemistry*. 70:669–678.

28. Robert Michaud, M., J.B. Benoit, G. Lopez-Martinez, M.A. Elnitsky, R.E. Lee, and D.L. Denlinger. 2008. Metabolomics reveals unique and shared metabolic changes in response to heat shock, freezing and desiccation in the Antarctic midge, Belgica antarctica. *J. Insect Physiol.* 54:645–655.

29. Crowley, K.J., and G. Zografi. 2001. The use of thermal methods for predicting glass-former fragility. *Thermochim. Acta*. 380:79–93.

30. Lewis, J.A., and J.T. Fleming. 1995. Basic culture methods. *Methods Cell Biol.* 48:3–29.

31. 2010. YPD media. *Cold Spring Harb. Protoc.* 2010:db.rec12315.

32. Dirama, T.E., G.A. Carri, and A.P. Sokolov. 2005. Role of hydrogen bonds in the fast dynamics of binary glasses of trehalose and glycerol: a molecular dynamics simulation study. *J. Chem. Phys.* 122:114505.

33. PubChem. Maltose. *https://pubchem.ncbi.nlm.nih.gov/compound/Maltose#section=Chemical-and-Physical-Properties*.

34. PubChem. Sucrose. *https://pubchem.ncbi.nlm.nih.gov/compound/Sucrose#section=Chemical-and-Physical-Properties*.

35. PubChem. Trehalose. *https://pubchem.ncbi.nlm.nih.gov/compound/Trehalose#section=Chemical-and-Physical-Properties*.

36. Chauhan, A. 2014. Powder XRD technique and its applications in science and technology. *J. Anal. Bioanal. Tech.* 5.

37. Madsen, I.C., N.V.Y. Scarlett, and A. Kern. 2011. Description and survey of methodologies for the determination of amorphous content via X-ray powder diffraction. *Zeitschrift für Kristallographie*. 226:944–955.

38. Piszkiewicz, S., K.H. Gunn, O. Warmuth, A. Propst, A. Mehta, K.H. Nguyen, E. Kuhlman, A.J. Guseman, S.S. Stadmiller, T.C. Boothby, S.B. Neher, and G.J. Pielak. 2019. Protecting activity of desiccated enzymes. *Protein Sci.* 28:941–951.

39. Goyal, K., L.J. Walton, and A. Tunnacliffe. 2005. LEA proteins prevent protein aggregation due to water stress. *Biochem. J.* 388:151–157.

40. Dyre, J.C. 2006. Colloquium: The glass transition and elastic models of glass-forming liquids. *Rev. Mod. Phys.* 78:953–972.

41. Rizzuto, M., A. Mugica, M. Zubitur, D. Caretti, and A.J. Müller. 2016. Plasticization and anti-plasticization effects caused by poly(lactide- ran -caprolactone) addition to double crystalline poly(l -lactide)/poly(ε-caprolactone) blends. *CrystEngComm*. 18:2014–2023.

42. Luk, E., A.J. Sandoval, A. Cova, and A.J. Müller. 2013. Anti-plasticization of cassava starch by

complexing fatty acids. *Carbohydr. Polym.* 98:659–664.

43. Chen, Y., T. Tang, and C. Ayranci. 2022. Moisture□induced anti□plasticization of polylactic acid: Experiments and modeling. *J. Appl. Polym. Sci.* 139:52369.

44. Figueroa, Y., M. Guevara, A. Pérez, A. Cova, A.J. Sandoval, and A.J. Müller. 2016. Effect of sugar addition on glass transition temperatures of cassava starch with low to intermediate moisture contents. *Carbohydr. Polym.* 146:231–237.

45. Liu, Y., A.K. Roy, A.A. Jones, P.T. Inglefield, and P. Ogden. 1990. An NMR study of plasticization and antiplasticization of a polymeric glass. *Macromolecules*. 23:968–977.

46. Tarique, J., S.M. Sapuan, and A. Khalina. 2021. Effect of glycerol plasticizer loading on the physical, mechanical, thermal, and barrier properties of arrowroot (Maranta arundinacea) starch biopolymers. *Sci. Rep.* 11:13900.

47. Matveev, Y.I., V.Y. Grinberg, and V.B. Tolstoguzov. 2000. The plasticizing effect of water on proteins, polysaccharides and their mixtures. Glassy state of biopolymers, food and seeds. *Food Hydrocoll.* 14:425–437.

48. Ruiz, G.N., M. Romanini, A. Hauptmann, T. Loerting, E. Shalaev, J.L. Tamarit, L.C. Pardo, and R. Macovez. 2017. Genuine antiplasticizing effect of water on a glass-former drug. *Sci. Rep.* 7:7470.

49. Combarro Palacios, I., C. Olsson, C.S. Kamma-Lorger, J. Swenson, and S. Cerveny. 2019. Motions of water and solutes-Slaving versus plasticization phenomena. *J. Chem. Phys.* 150:124902.

50. Baud, S., J.-P. Boutin, M. Miquel, L. Lepiniec, and C. Rochat. 2002. An integrated overview of seed development in Arabidopsis thaliana ecotype WS. *Plant Physiol. Biochem.* 40:151–160.

51. Janis, B., C. Belott, and M.A. Menze. 2018. Role of Intrinsic Disorder in Animal Desiccation Tolerance. *Proteomics*. 18:e1800067.

52. Erkut, C., S. Penkov, H. Khesbak, D. Vorkel, J.-M. Verbavatz, K. Fahmy, and T.V. Kurzchalia. 2011. Trehalose renders the dauer larva of Caenorhabditis elegans resistant to extreme desiccation. *Curr. Biol.* 21:1331–1336.

53. Calahan, D., M. Dunham, C. DeSevo, and D.E. Koshland. 2011. Genetic analysis of desiccation tolerance in Sachharomyces cerevisiae. *Genetics*. 189:507–519.

54. Walters, C. 2004. Temperature dependency of molecular mobility in preserved seeds. *Biophys. J.* 86:1253–1258.

55. Ballesteros, D., and C. Walters. 2011. Detailed characterization of mechanical properties and molecular mobility within dry seed glasses: relevance to the physiology of dry biological systems. *Plant J.* 68:607–619.

56. Walters, C. 1998. Understanding the mechanisms and kinetics of seed aging. *Seed Sci. Res.* 8:223–244.

57. Leprince, O., and C. Walters-Vertucci. 1995. A Calorimetric Study of the Glass Transition Behaviors in Axes of Bean Seeds with Relevance to Storage Stability. *Plant Physiol.* 109:1471–1481.

Acknowledgments

This work was primarily supported by NSF DBI grant # 2213983. This work was partially funded through a fellowship to JFR administered by Wyoming NASA EPSCoR (NASA Grant #80NSSC19M0061). JFR is supported by the USDA National Institute of Food and Agriculture, Hatch project #1012152. The authors gratefully acknowledge financial support from the NSF (CHE 0619920 to NA and IntBio 2128069 to TCB) and the Institutional Development Award (IDeA) from the National Institute of General Medical Sciences of the National Institutes of Health (Grant # 2P20GM103432). Any opinions, findings, conclusions, or recommendations expressed in this publication are those of the author(s) and do not necessarily reflect the view of the National Institute of Food and Agriculture (NIFA) or the United States Department of Agriculture (USDA). *Arabidopsis thaliana* adult plant leaves were donated by the Park Laboratory at the University of Wyoming, department of Molecular Biology. *Caenorhabditis elegans daf-2* strains were donated by the Fay Laboratory at the University of Wyoming, department of Molecular biology. *Saccharomyces cerevisiae* strain BY4742 was donated by Dr. Peter Thorsness Emeritus Professor at the University of Wyoming, department of Molecular Biology. We thank members of the Water and Life Interface Institute (WALII), supported by NSF DBI grant # 2213983, in particular Christina Walters, for helpful discussions.The authors are thankful to Dr. Silvia Sanchez Martinez and members of the Boothby Lab for discussions and reading of this manuscript.

Author contributions

John F. Ramirez: Conceptualization, Methodology, Investigation, Formal analysis, Data curation, Writing - Original Draft, Writing - Review and Editing, Visualization. **U.G.V.S.S. Kumara:** Methodology, Investigation, Data Curation, Writing - Review and Editing. **Navamoney Arulsamy:** Investigation, Writing - Original Draft, Writing - Review and Editing. **Thomas C. Boothby:** Conceptualization, Methodology, Writing - Original Draft, Writing - Review and Editing, Supervision, Visualization, Project administration, Funding acquisition.

Declaration of Interests

The authors declare no competing interests.

Data availability statement

The raw data required to reproduce these findings are available to download from https://data.mendeley.com/datasets/bwmrgpg49x/draft?a=a5218f9e-56b6-4413-aa1c-95c7bdbb98fc. The processed data required to reproduce these findings are available to download from https://data.mendeley.com/datasets/bwmrgpg49x/draft?a=a5218f9e-56b6-4413-aa1c-95c7bdbb98fc.

Additional information

The authors declare no competing interests.

Figures and Figure legends

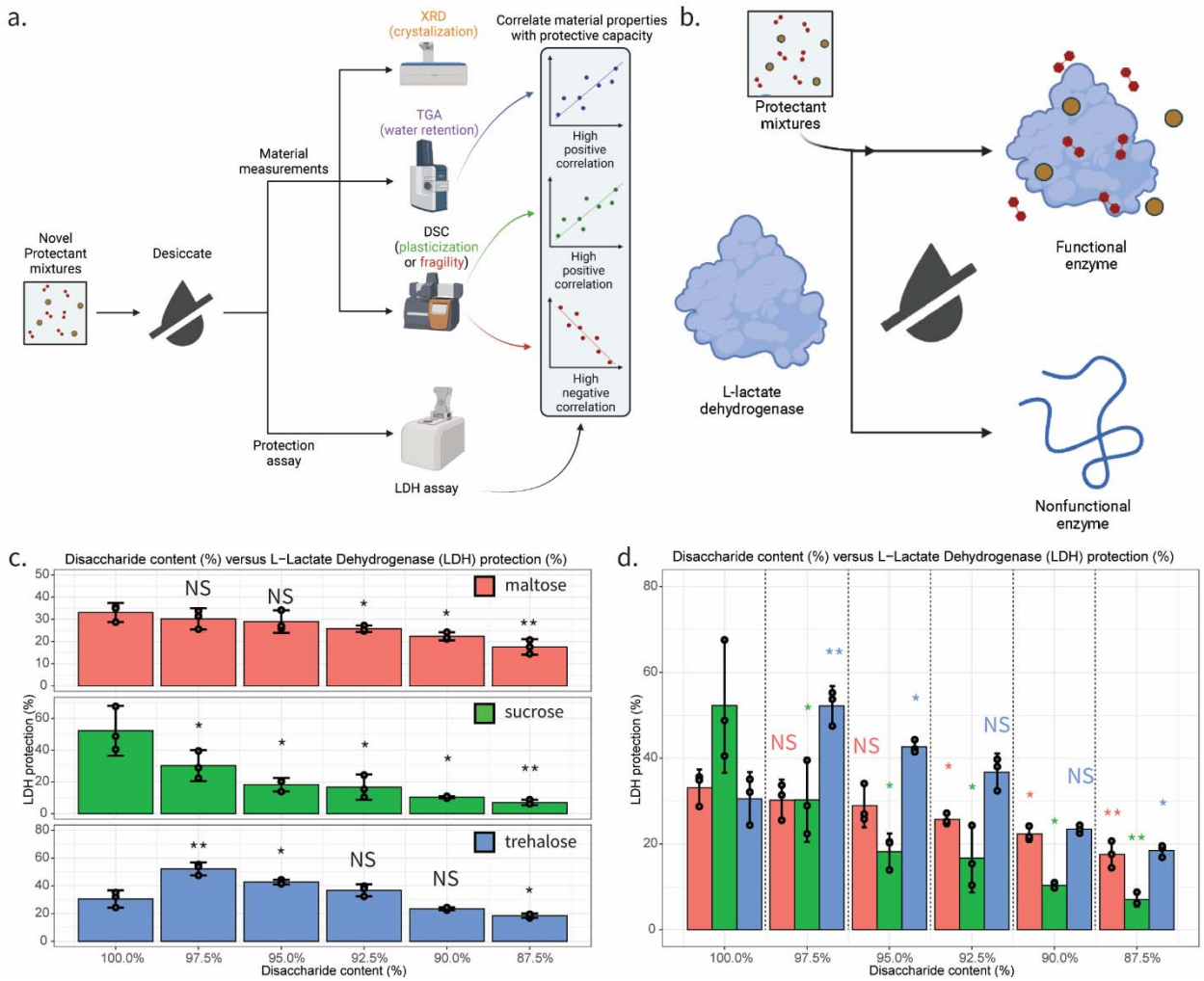

Figure 1: Vitrified disaccharide-glycerol mixtures display variable protective properties. a) Schematic overview of workflow to produce correlation values between material properties and enzyme protective capacity. b) Schematic demonstrating how an LDH assay will evaluate enzyme functionality. c) Lactate dehydrogenase (LDH) enzyme protection values for disaccharide-glycerol mixtures organized by disaccharide. d) LDH enzyme protection values for disaccharide-glycerol mixtures organized by disaccharide content, p-value ≤ 0.05 (*) p-value ≤ 0.01 (**), p-value ≤ 0.001 (***), NS is not significant, error bars represent 95% CI.

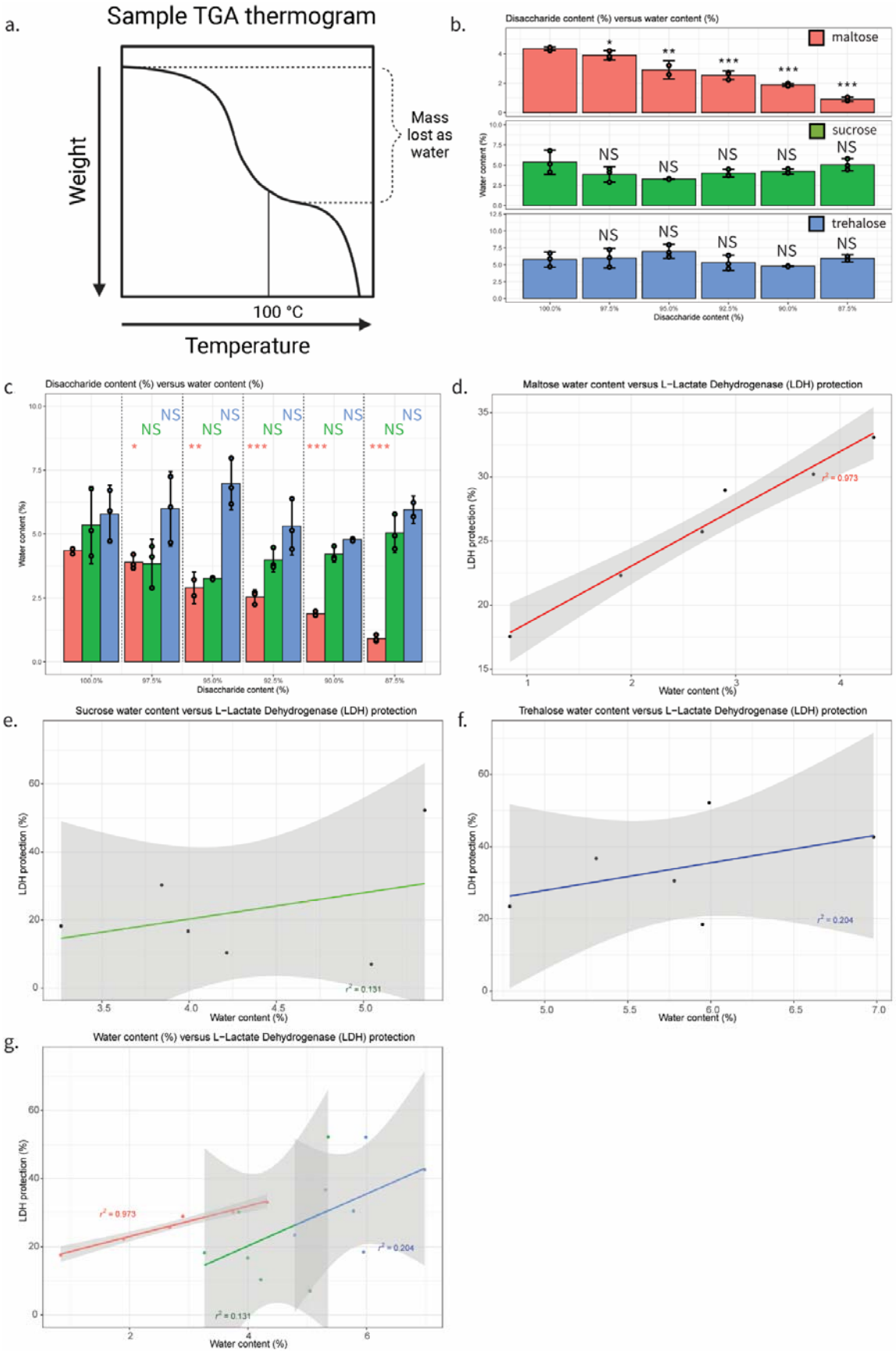
a.
Sample TGA thermogram
Weight
Mass lost as water
100 °C
Temperature
b.
Disaccharide content (%) versus water content (%)
maltose
sucrose
trehalose
Water content (%)
Disaccharide content (%)
c
Disaccharide content (%) versus water content (%)
Water content (%)
Disaccharide content (%)
d.
Maltose water content versus L−Lactate Dehydrogenase (LDH) protection
LDH protection (%)
Water content (%)
e.
Sucrose water content versus L−Lactate Dehydrogenase (LDH) protection
LDH protection (%)
Water content (%)
f.
Trehalose water content versus L−Lactate Dehydrogenase (LDH) protection
LDH protection (%)
Water content (%)
g.
Water content (%) versus L−Lactate Dehydrogenase (LDH) protection
LDH protection (%)
Water content (%)

Figure 2: Water content correlates with the protective capacity of maltose-glycerol but not sucrose- or trehalose-glycerol glasses. a) Schematic representation of an idealized TGA thermogram highlighting region of mass lost as water. b) Water content values for disaccharide-glycerol mixtures organized by disaccharide. c) Water content values for disaccharide-glycerol mixtures organized by disaccharide content. d) Correlation plot of water content versus protection for maltose-glycerol mixtures. e) Correlation plot of water content versus protection for sucrose-glycerol mixtures. f) Correlation plot of water content versus protection for trehalose-glycerol mixtures. g) Correlation plot of water content versus protection for all disaccharide-glycerol mixtures, p-value ≤ 0.05 (*) p-value ≤ 0.01 (**), p-value ≤ 0.001 (***), NS is not significant (statistical comparisons in b and c are made against 100% for each sugar series), n = 3, error bars represent 95% CI.

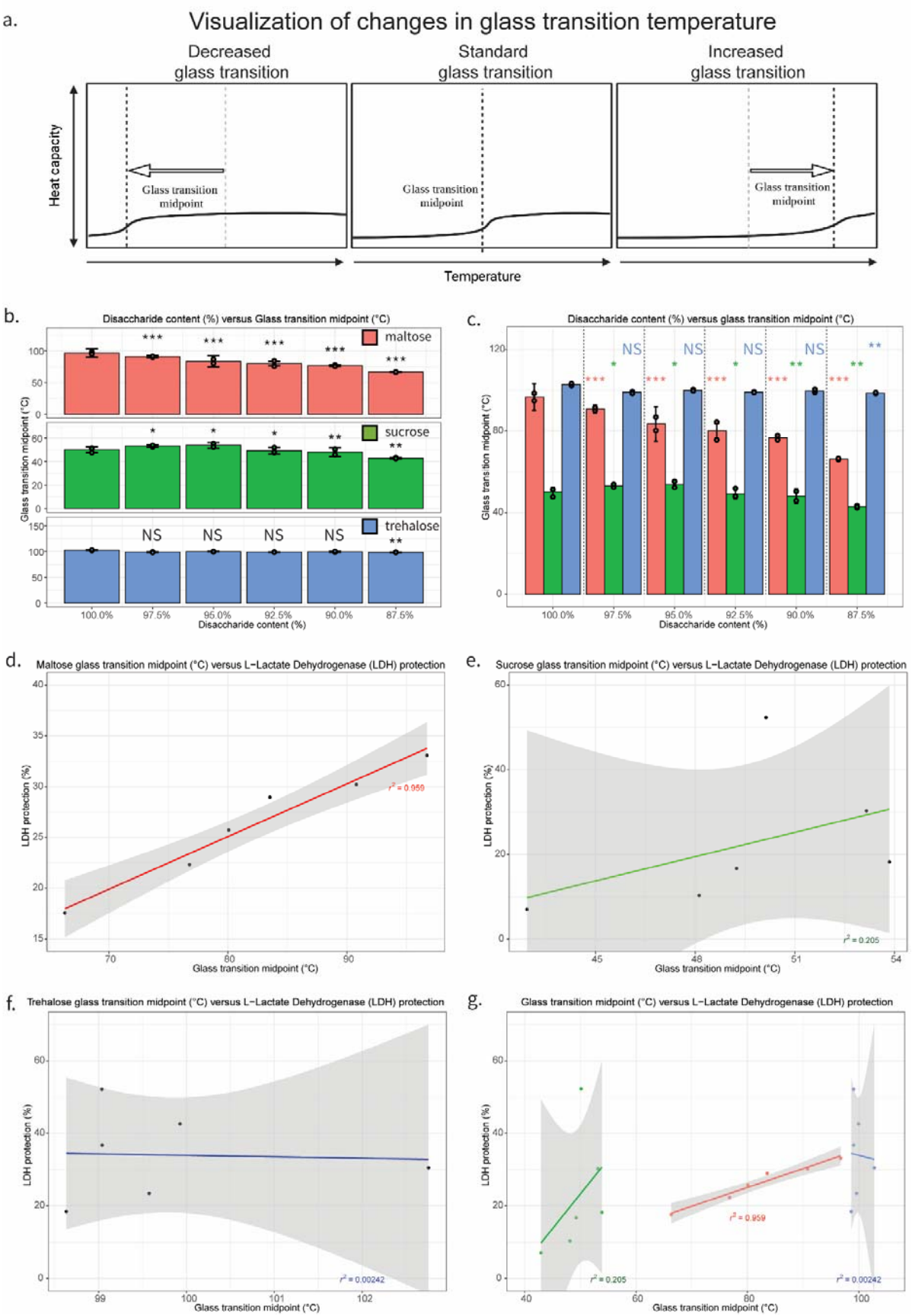
a.
Visualization of changes in glass transition temperature
Decreased glass transition
Standard glass transition
Increased glass transition
Heat capacity
Glass transition midpoint
Temperature
b.
Disaccharide content (%) versus Glass transition midpoint (°C)
maltose
sucrose
trehalose
Glass transition midpoint (°C)
Disaccharide content (%)
c.
Disaccharide content (%) versus glass transition midpoint (°C)
Glass transition midpoint (°C)
Disaccharide content (%)
d.
Maltose glass transition midpoint (°C) versus L−Lactate Dehydrogenase (LDH) protection
LDH protection (%)
Glass transition midpoint (°C)
e.
Sucrose glass transition midpoint (°C) versus L−Lactate Dehydrogenase (LDH) protection
LDH protection (%)
Glass transition midpoint (°C)
f.
Trehalose glass transition midpoint (°C) versus L−Lactate Dehydrogenase (LDH) protection
LDH protection (%)
Glass transition midpoint (°C)
g.
Glass transition midpoint (°C) versus L−Lactate Dehydrogenase (LDH) protection
LDH protection (%)
Glass transition midpoint (°C)

Figure 3: Anti-plasticization of maltose- and sucrose-, but not trehalose-glycerol glasses correlate with protection. a) Schematic representation of an idealized DSC thermogram illustrating a decrease or increase in glass transition midpoint. b) Glass transition midpoint values for disaccharide-glycerol mixtures organized by disaccharide. c) Glass transition midpoint values for disaccharide-glycerol mixtures organized by disaccharide content. d) Correlation plot of glass transition midpoint versus protection for maltose-glycerol mixtures. e) Correlation plot of glass transition midpoint versus protection for sucrose-glycerol mixtures. f) Correlation plot of glass transition midpoint versus protection for trehalose-glycerol mixtures. g) Correlation plot of glass transition midpoint versus protection for all disaccharide-glycerol mixtures, p-value ≤ 0.05 (*) p-value ≤ 0.01 (**), p-value ≤ 0.001 (***), NS is not significant, (statistical comparisons in b and c are made against 100% for each sugar series), n = 3, error bars represent 95% CI.

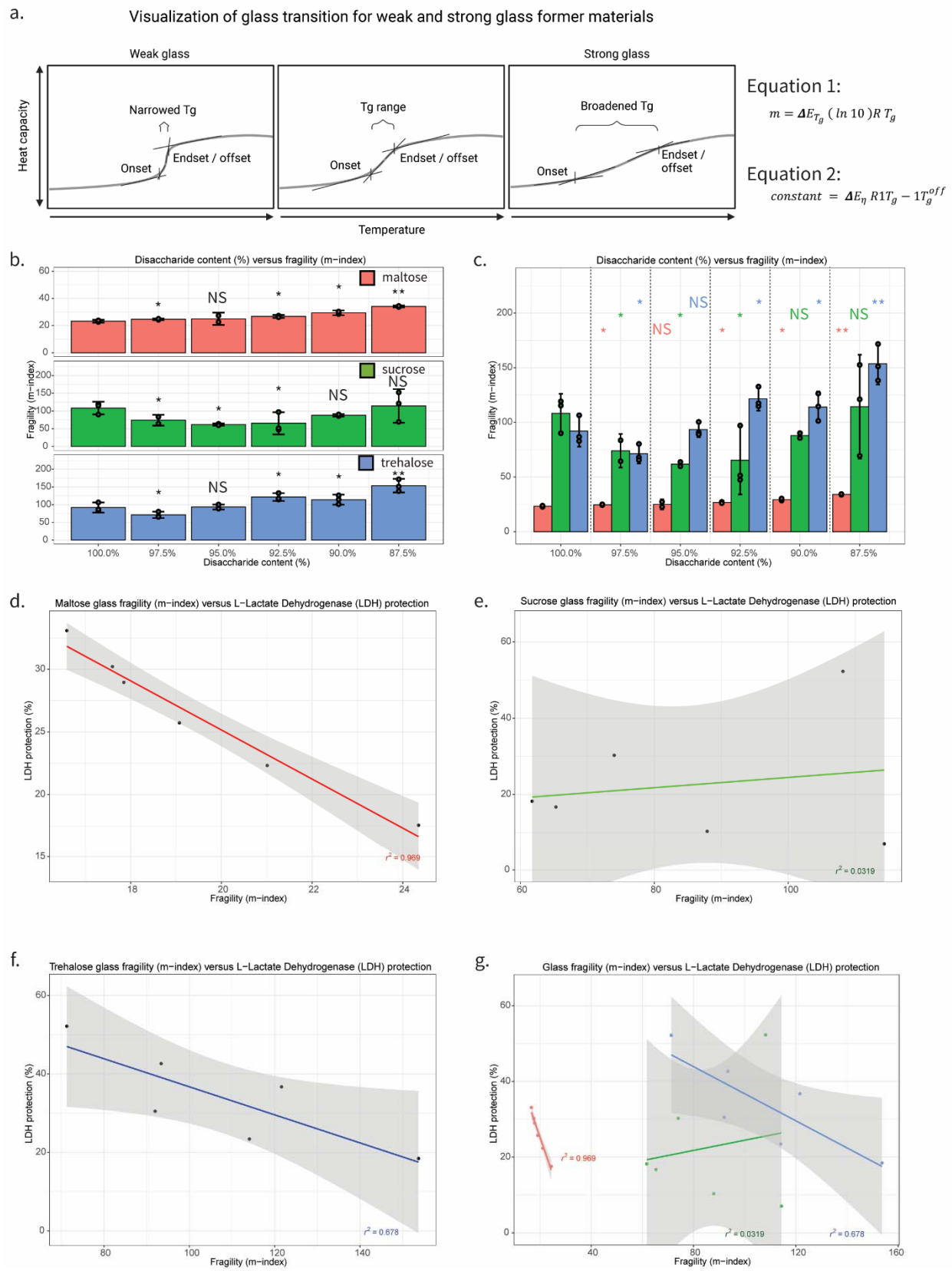

Figure 4: Reduced glass forming fragility of maltose- and trehalose-, but not sucrose-glycerol glasses correlates with protection. a) Schematic representation of idealized DSC thermograms illustrating a

narrowing or broadening of the glass transition and the two equations used to calculate m-index. b) Glass former fragility (m-index) values for disaccharide-glycerol mixtures organized by disaccharide. c) Glass former fragility (m-index) values for disaccharide-glycerol mixtures organized by disaccharide content. d) Correlation plot of glass former fragility (m-index) versus protection for maltose-glycerol mixtures. e) Correlation plot of glass former fragility (m-index) versus protection for sucrose-glycerol mixtures. f) Correlation plot of glass former fragility (m-index) versus protection for trehalose-glycerol mixtures. g) Correlation plot of glass former fragility (m-index) versus protection for all disaccharide-glycerol mixtures, p-value ≤ 0.05 (*) p-value ≤ 0.01 (**), p-value ≤ 0.001 (***), NS is not significant (statistical comparisons in b and c are made against 100% for each sugar series), n = 3, error bars represent 95% CI.

	Water content (%)	Tg onset
	4.35 +/- 0.12	70.80 +/- 2.06
	3.90 +/- 0.31	66.86 +/- 1.89
	2.90 +/- 0.62	60.22 +/- 10.59
	2.53 +/- 0.29	58.74 +/- 8.92
	1.89 +/- 0.09	57.69 +/- 0.68
	0.91 +/- 0.15	50.46 +/- 1.01
	5.35 +/- 1.50	46.80 +/- 2.09
	3.84 +/- 1.17	48.21 +/- 0.10
	3.27 +/- 0.06	47.99 +/- 3.22
	3.99 +/- 0.47	43.19 +/- 1.97
	4.22 +/- 0.38	44.10 +/- 4.61
	5.05 +/- 0.77	39.56 +/- 1.89
	5.78 +/- 1.13	98.21 +/- 1.25
	5.99 +/- 1.46	93.24 +/- 1.09
	6.98 +/- 1.45	95.53 +/- 0.36
	5.31 +/- 1.13	95.67 +/- 0.24
	4.79 +/- 0.05	95.96 +/- 0.39
	5.95 +/- 0.54	95.97 +/- 0.11

Table 1: *In vitro* measurement results organized by disaccharide-glycerol content and by material property, error values represent 95% CI.

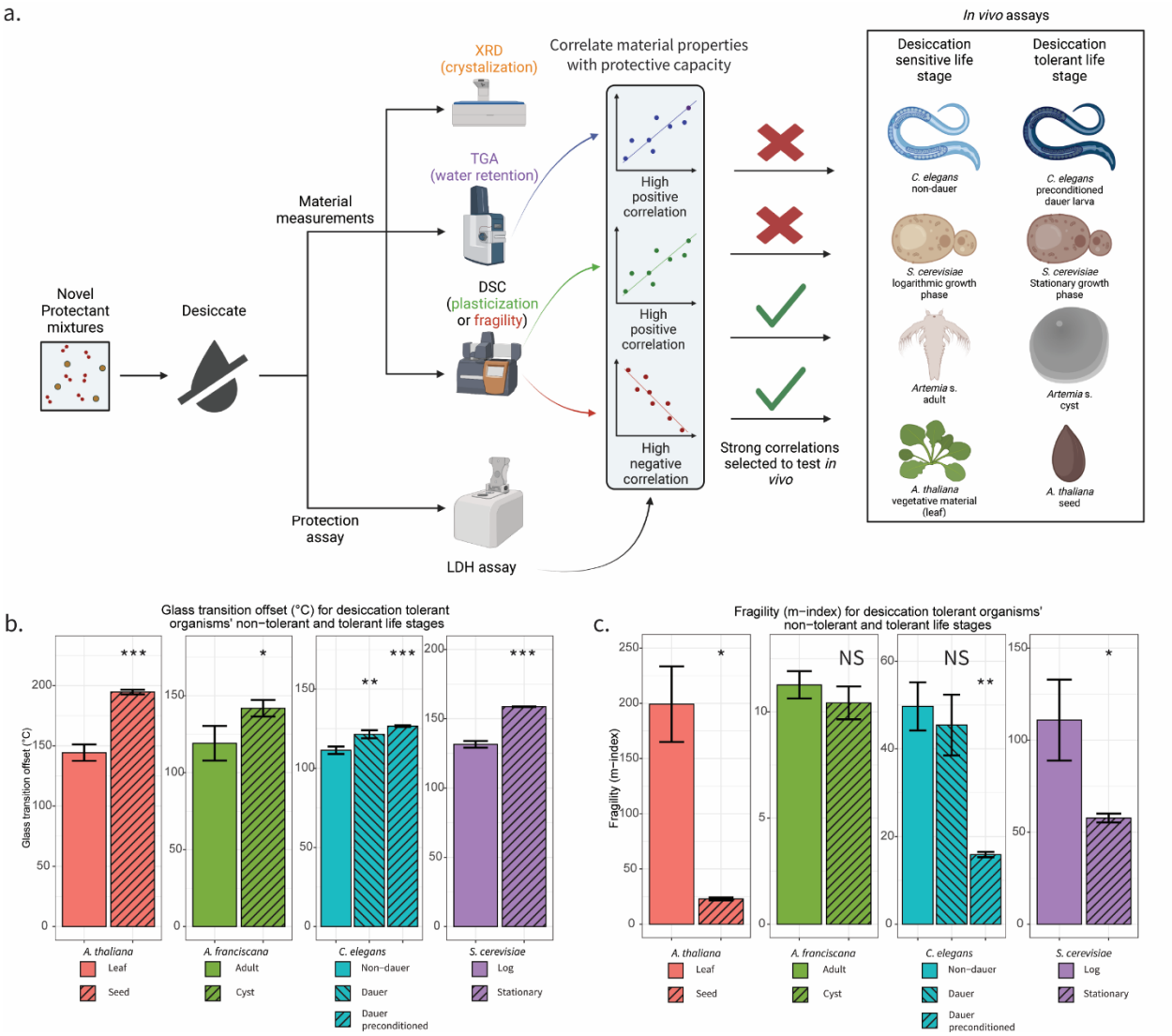

Figure 5: *In vivo* glass transition temperature is increased and glass former fragility reduced in desiccation-tolerant *versus* sensitive life stages of diverse anhydrobiotic organisms. a) Schematic representation of our workflow illustrating how material properties were selected to be tested with in vivo assays. b) Glass transition offset values for selected desiccation tolerant organisms organized by organism and life stage. c) Glass former fragility (m-index) values for selected desiccation tolerant organisms organized by organism and life stage, p-value $\leq< 0.05$ (*) p-value $\leq< 0.01$ (**), p-value $\leq< 0.001$ (***), NS is not significant (statistical comparisons in b and c are made against 100% for each sugar series), n = 3, error bars represent 95% CI.

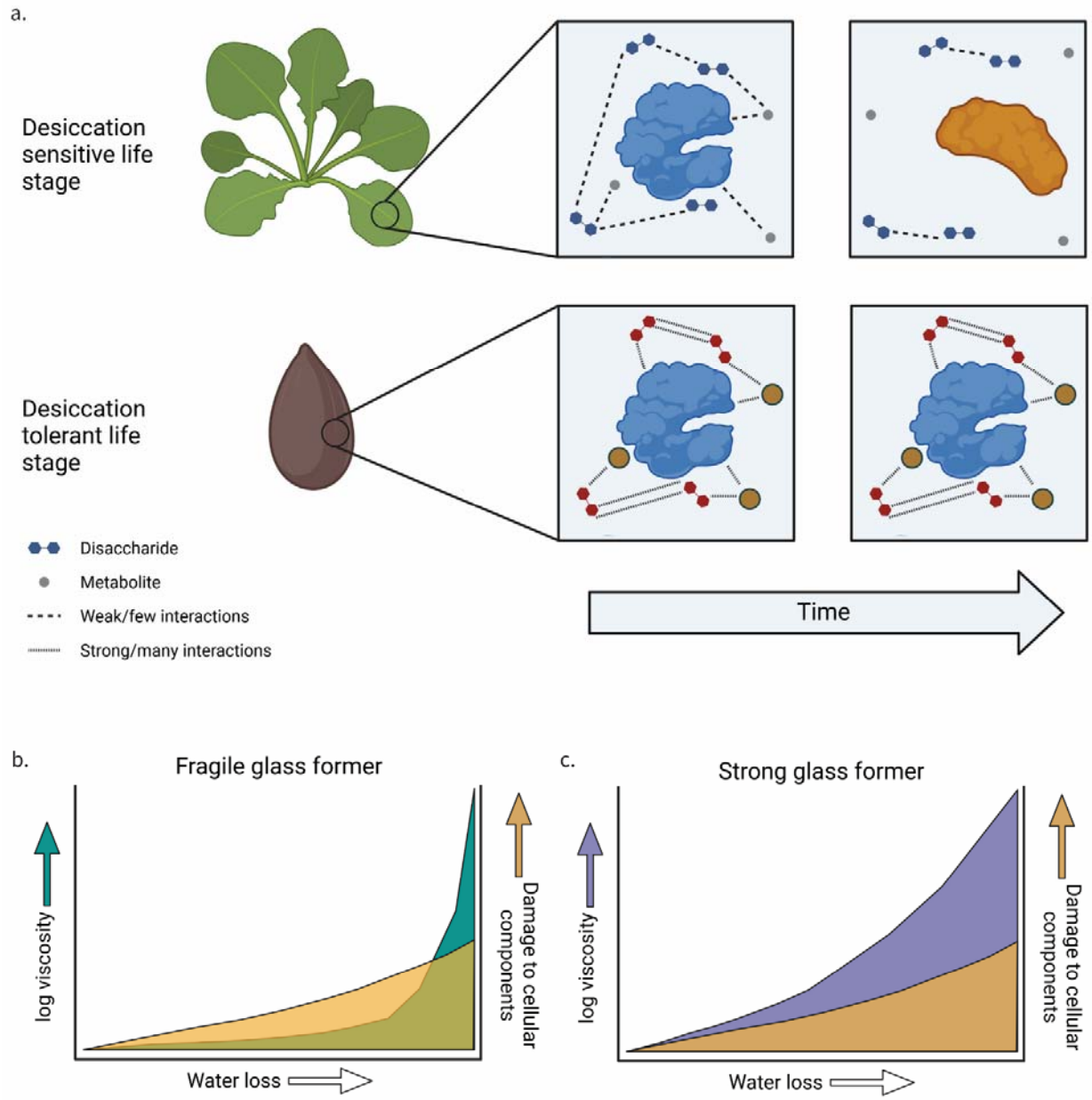

Figure 6: Model of protection conferred by increased glass transition temperature and reduced glass former fragility. a) Schematic representation of the potential mechanism of protection conferred by increasing glass transition temperature. b) Schematic representation of the potential mechanism underlying how damage is accrued in fragile glass former mixtures. c) Schematic of the potential mechanism underlying how damage is prevented in strong glass former systems.

Supplemental figures:

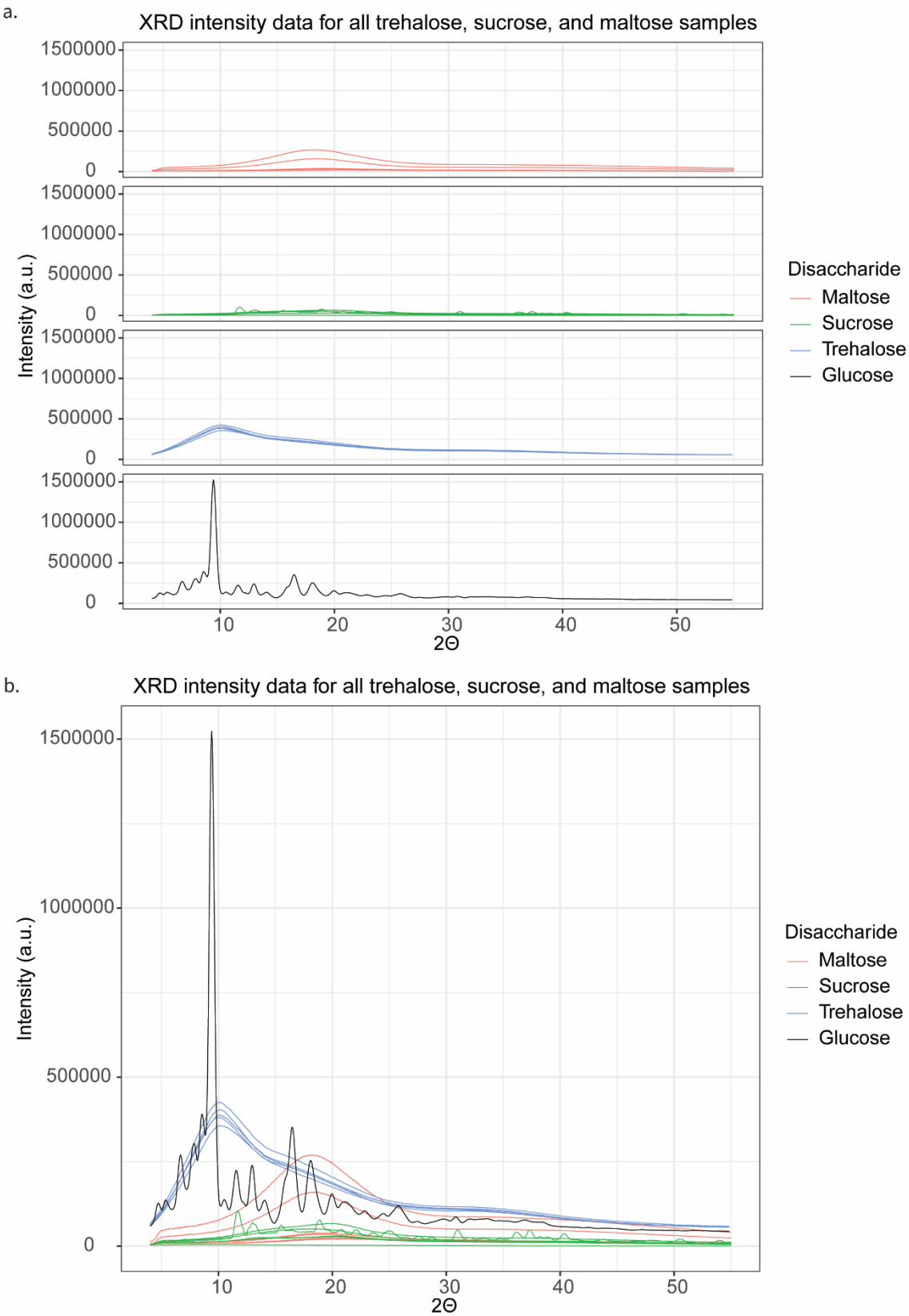

Figure S1: *In vitro* disaccharide-glycerol mixtures produce non-crystalline amorphous ("glassy") solids when desiccated. a) XRD intensity (a.u.) values for disaccharide-glycerol mixtures organized by

disaccharide. b) XRD intensity (a.u.) values for disaccharide-glycerol mixtures organized by disaccharide content.

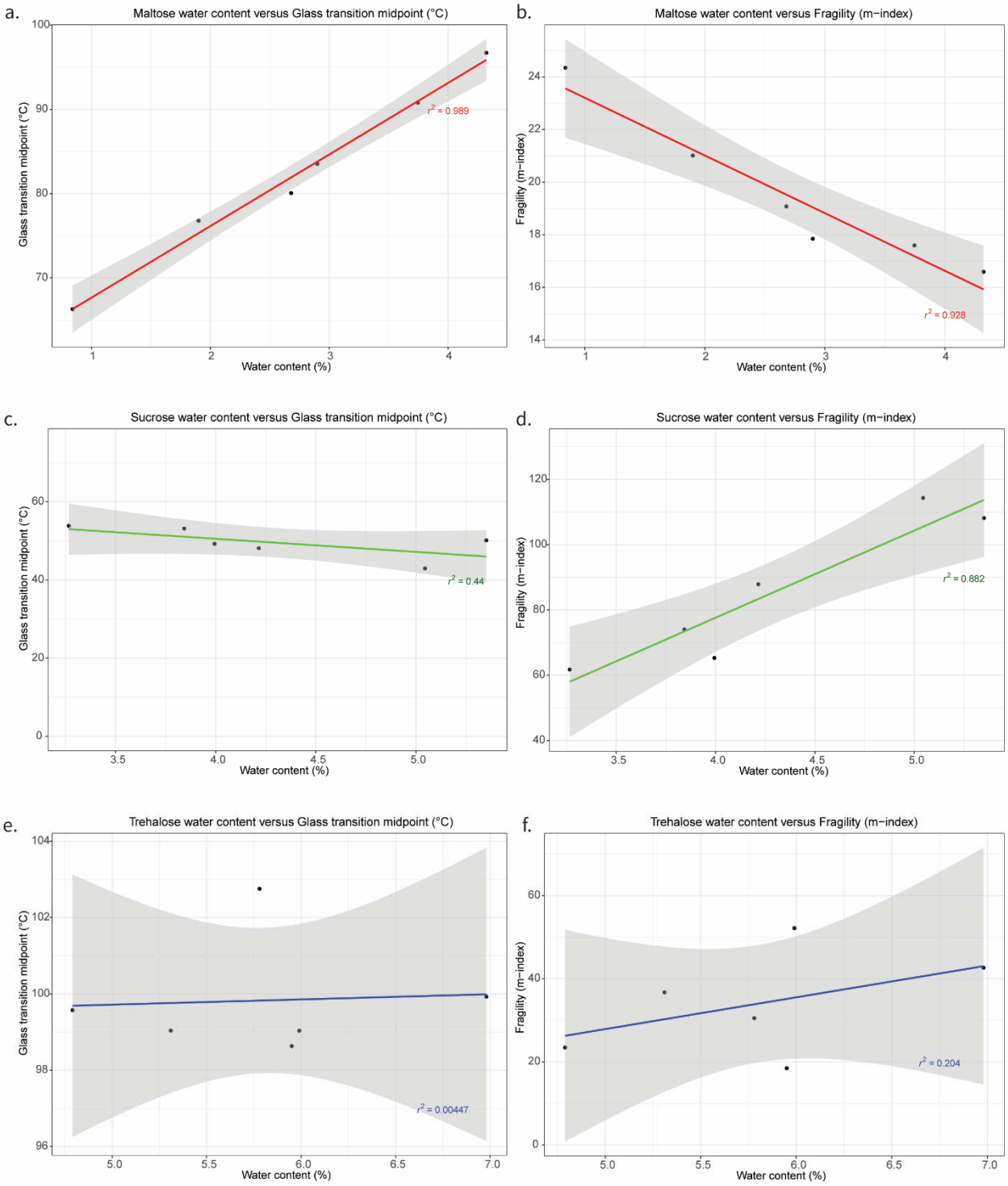

Figure S2: Water content appears to correlate with other material properties for some disaccharide-glycerol mixtures. a) Correlation plot of water content versus glass transition midpoint for maltose-glycerol mixtures. b) Correlation plot of water content versus fragility (m-index) for maltose-glycerol mixtures. c) Correlation plot of water content versus glass transition midpoint for sucrose-glycerol mixtures. d) Correlation plot of water content versus fragility (m-index) for sucrose-glycerol mixtures. e) Correlation plot of water content versus glass transition midpoint for trehalose-glycerol mixtures. f)

Correlation plot of water content versus fragility (m-index) for trehalose-glycerol mixtures, error bars represent 95% CI.

a.

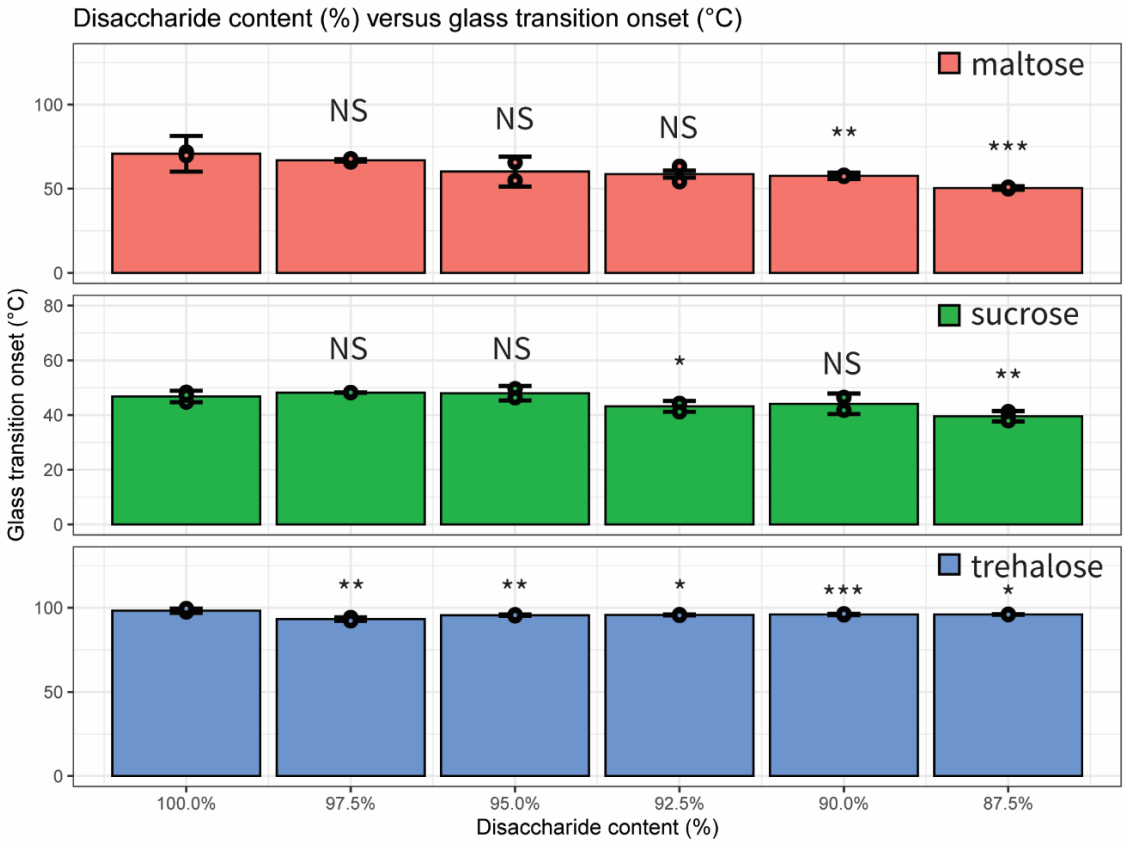
Disaccharide content (%) versus glass transition onset (°C)
maltose
sucrose
trehalose
NS
*
**
***
Glass transition onset (°C)
100.0%
97.5%
95.0%
92.5%
90.0%
87.5%
Disaccharide content (%)

b.

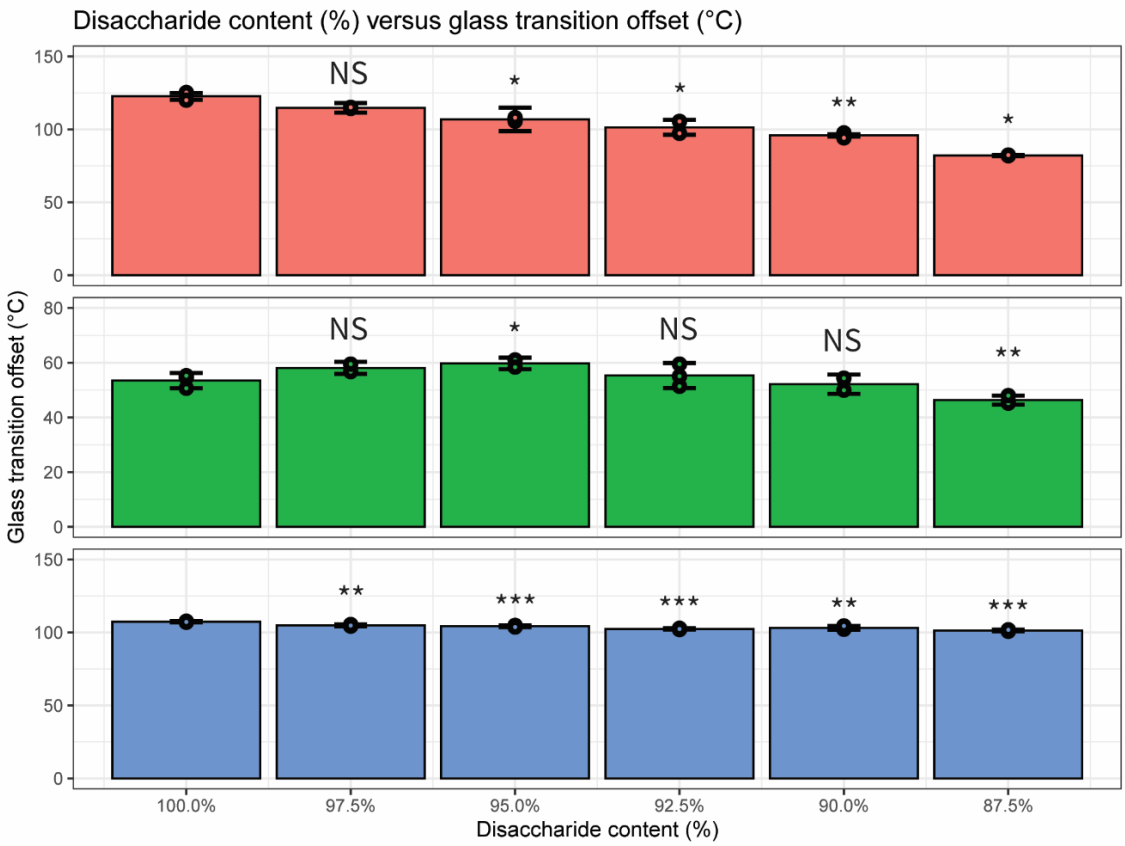
Disaccharide content (%) versus glass transition offset (°C)
NS
*
**
***
Glass transition offset (°C)
100.0%
97.5%
95.0%
92.5%
90.0%
87.5%
Disaccharide content (%)

Figure S3: Glass transition onset and offset vary by disaccharide-glycerol mixtures differently than the glass transition midpoint. a) Glass transition onset values for disaccharide-glycerol mixtures organized by disaccharide. b) Glass transition offset values for disaccharide-glycerol mixtures organized by disaccharide, p-value $\leq$ 0.05 (*) p-value $\leq$ 0.01 (**), p-value $\leq$ 0.001 (***), NS is not significant (statistical comparisons in a and b are made against 100% for each sugar series), n = 3, error bars represent 95% CI.

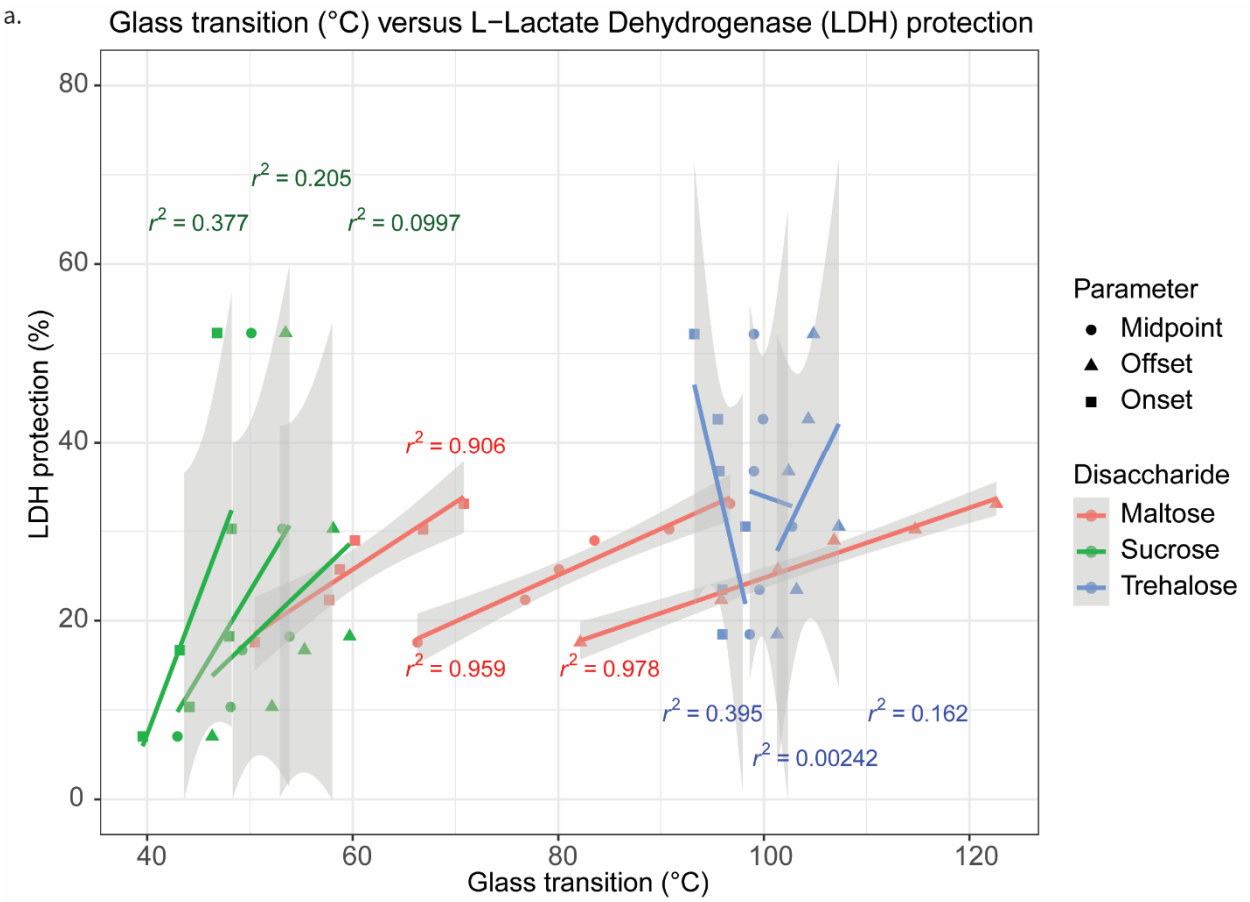

Figure S4: Glass transition onset, midpoint, and offset are better correlated with protection for different disaccharide-glycerol mixtures. a) Correlation plot of glass transition onset, midpoint, and offset versus protection for maltose-, sucrose-, and trehalose-glycerol mixtures, error bars represent 95% CI.